



HAL
open science

Dynamic heat transfer modeling of a closed refrigerated display cabinet

N. Chaomuang, Onrawee Laguerre, D. Flick

► **To cite this version:**

N. Chaomuang, Onrawee Laguerre, D. Flick. Dynamic heat transfer modeling of a closed refrigerated display cabinet. Applied Thermal Engineering, 2019, 161, pp.17. 10.1016/j.applthermaleng.2019.114138 . hal-02609583

HAL Id: hal-02609583

<https://hal.inrae.fr/hal-02609583>

Submitted on 21 Dec 2021

HAL is a multi-disciplinary open access archive for the deposit and dissemination of scientific research documents, whether they are published or not. The documents may come from teaching and research institutions in France or abroad, or from public or private research centers.

L'archive ouverte pluridisciplinaire **HAL**, est destinée au dépôt et à la diffusion de documents scientifiques de niveau recherche, publiés ou non, émanant des établissements d'enseignement et de recherche français ou étrangers, des laboratoires publics ou privés.



Distributed under a Creative Commons Attribution - NonCommercial 4.0 International License

1

2 **Heat properties of a hydrophilic carboxylate-based MOF for**
3 **water adsorption applications**

4

5 Shuqing Cui^a, Afsaneh Marandi^b, Gaëlle Lebourleux^c, Mireille Thimon^c, Maxime Bourdon^c,

6 Chaoben Chen^a, Maria Inês Severino^b, Victoria Steggles^b, Farid Nouar^b, Christian Serre^{b*}

7

^aElektron Gri, 10 rue des trois portes, 75005 Paris, France

8

^bInstitut des Matériaux Poreux de Paris, UMR 8004 CNRS, Ecole Normale Supérieure,

9

Ecole Supérieure de Physique et de Chimie Industrielles de Paris, PSL University, 75005

10

Paris, France

11

^cSetaram Instrumentation, 7 rue de l'Oratoire, 69300 Caluire, France

12

*Corresponding author's email:

13

christian.serre@ens.fr

14

15

16

17

18

19

20

21

22

23

24

25 **Abstract**

26 The development of new porous materials is expanding the boundaries of applications
27 related to gas adsorption, including gas separation, catalysis, drying and energy storage.
28 The specific heat capacity and thermal conductivity of the adsorbent materials are
29 important parameters in the engineering process. For instance, in the adsorptive heat pump
30 technology, the energy generation and transfer by the adsorbent during the adsorption and
31 desorption process of the adsorbate directly determines the energy efficiency of the
32 working cycle. However, the thermal properties' data for the novel types of adsorbent
33 materials, metal-organic frameworks (MOF), is often lacking in the literature. This work
34 followed a protocol particularly relevant for the measurement of MOFs' thermal properties
35 under powder form. A very promising hybrid material for energy storage, separation and
36 other applications, MIL-160, has been tested as a reference. The specific heat capacity of
37 the material was measured at temperatures ranging from 20 °C to 75 °C with a heat flow
38 type differential scanning calorimeter (DSC). The thermal conductivity was measured with
39 a transient heating source technique within a similar temperature range. By fitting the
40 experimental data to the Clausius-Clapeyron model, the performance of this material in the
41 application of adsorptive heat pump was obtained.

42

43

44

45

46 **Key words**

47 Metal-organic frameworks, specific heat capacity, thermal conductivity, adsorption,
48 thermodynamic efficiency

49

50 **Introduction**

51 The superior adsorption performance of modern porous solid materials incited the
52 development of various technologies including gas storage and separation,
53 dehumidification, cooling, and heating. In an adsorption process, the guest molecules
54 attach to adsorption sites on the surface of the host molecules, creating a relatively stable
55 phase by interactions of chemical bonds between the adsorbate and the adsorbent. The
56 adsorbent can later release the adsorbate when receiving external energy input. The whole
57 process involves a large amount of energy conversion under heat form, while porous solids
58 often have high specific heat capacity and low thermal conductivity due to open pore
59 structure and high pore volume, which often lead to a reduction in the sorption
60 performance.

61 As a new class of porous solids, metal-organic frameworks have aroused a great interest for
62 its potential in the immense possibilities of fine-tuned adsorptive properties [1]. Also, water
63 has been considered as the best green sorbate due to its broad applicability, non-toxicity
64 and large enthalpy during sorption. Since the discovery of water-stable MOFs, the
65 adsorption applications based on water-MOFs pairs have promoted cross-border research
66 between fundamental chemistry and thermal engineering [2][3][4]. The unique functions of
67 MOFs in tuning the hydrophilicity and water uptake show prospects in the improvement of
68 energy efficiency in specific working environment [5]. Variable concepts have made
69 progress in the aforementioned applications, especially in cooling [6][7][8], water
70 production[9][10][11][12] and drying[13][14][15].

71 The pore-filling step of water in MOF for the adsorption application in practice should be
72 reversible. Water molecules interact with the polar sites in MOF's structure via hydrogen
73 bonds, but not via strong coordination bonds within the frameworks. This pore-filling
74 mechanism is different from a typical chemisorption and can have a smaller adsorption
75 enthalpy close to the water evaporation heat. As a consequence, a strategy of developing
76 novel sorbents is to create ordered large pores to enhance the cyclic adsorption capacity
77 [16][17]. A higher fraction of void volume would result in undesirable heat properties that
78 have a negative impact on the cycling sorption performance.

79 The charging and discharging of thermal energy accompanying the cyclic ad-desorption
80 operations involves heat retention by the sorbents and thus a rapid temperature swing of the
81 MOFs. Because a miniscule movement along the step-wise sorption isotherms of MOFs
82 may engender a great amount of change in water uptake, precise measurement of specific

83 heat capacity and thermal conductivity has a significant impact on the evaluation and
84 prediction of the adsorption performance, especially in a dynamic modeling work. Yet very
85 few values have been reported in the literature and most researchers adopt an average heat
86 capacity of 1 J/(g. K). Huang et al.[18] have reported a thermal conductivity below 0.1 W/
87 m K of MOF-5 at room temperature after shaping, which is much lower than the single
88 crystal. Purewal et al. [19] have showed that this value can increase by 5 times with 10wt%
89 graphite additives. Ming et al. [20] measured the specific heat capacity of MOF-5 as 0.72
90 J/g K, similar to alumina and graphite. Erickson KJ et al.[21] found HKUST-1 composite
91 with a thermal conductivity of 0.27 W/ m K. These results remain in the range of low heat
92 transfer performance similar to conventional adsorbents such as zeolite type X, zeolite type
93 CHA, carbon- or silica-based matrix encapsulating phase change materials (PCM),
94 etc.[22][23][24][25][26][27]

95 The differential scanning calorimetry is a dominant technique in the direct measurement of
96 heat properties for its simple operation and wide adaptability to variable working
97 conditions [28]. Frazzica et al. [29] developed a methodology to directly measure the heat
98 transfer properties of AQSOA Z02 in an adsorptive heat pump application with similar
99 techniques. BASF and co-workers [30] carried out the room temperature thermal
100 conductivity test of MOF-5 for gas storage by a DSC and a xenon thermal flash diffusivity
101 instrument. Mu and Walton [31] measured the specific heat capacity of several MOFs by
102 using DSC coupled with a thermal gravimetric analyzer covering 50 to 200 °C to verify
103 their thermal stability.

104 In this work, a simple method and protocol is presented for the measurement of heat
105 transfer properties of MOF bulk materials for adsorption applications. The specific heat
106 capacity and thermal conductivity are key parameters in the design of adsorptive based
107 energy transformation devices. A hydrophilic Al furane dicarboxylic based MOF,
108 MIL-160(Al), which is one of the most promising adsorbents to date in the storage and
109 transformation of low-grade energy is taken as an example [32]. The thermal efficiency of
110 an adsorptive heat pump employing the adsorbent is also derived.

111 **1. Experiments**

112 1.1 Material preparation

113 MIL-160(Al) was synthesized via an up-scale version of the process reported in a previous
114 study [32]. In short, Al(OH)(CH₃COO)₂ (0.6 mol, 93.7 g; Aldrich, 90%) and

115 2,5-furandicarboxylic acid (0.6 mol, 97.3 g) were mixed in distilled water (600 mL) and
116 stirred under reflux condition for 24 h. The mixture was filtered and washed with ethanol at
117 room temperature. The resulting white solid in powder form was dried under 100°C,
118 yielding 111.5g activated MIL-160(Al) (90%).

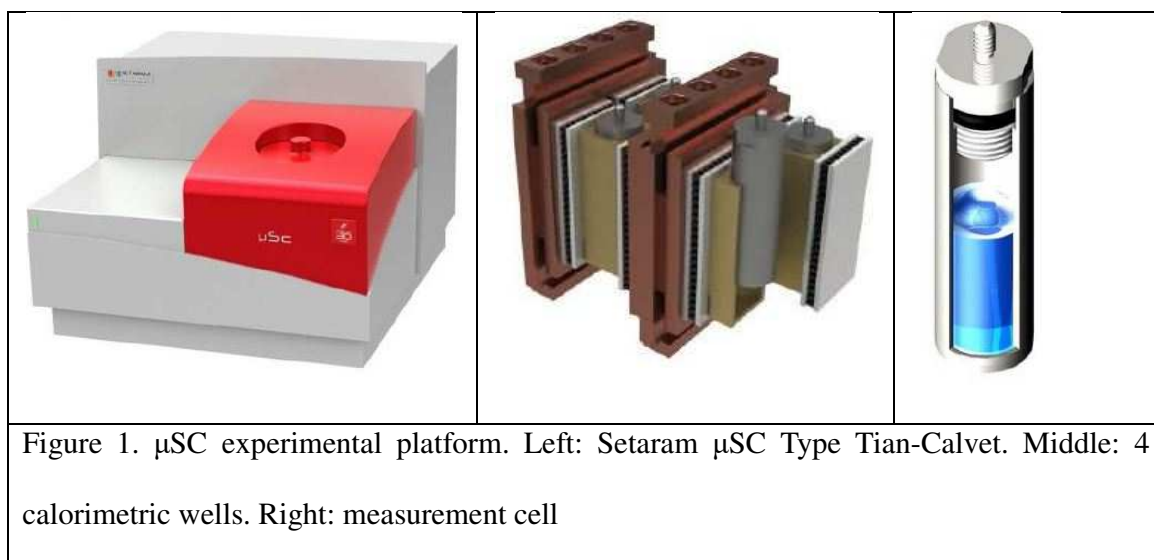
119 The Brunauer-Emmett-Teller (BET) surface calculations were carried out from N₂
120 adsorption-desorption isotherms measured at liquid nitrogen temperature (77 K) after
121 dehydration under vacuum at 423 K for 12 h using Micromeritics Tristar 3020. The pore
122 volume was taken by a single point method at relative pressure (p/p_0) = 0.99. The
123 high-resolution X-ray powder diffraction-pattern of MIL-160 was recorded in two hours
124 within the 4-60 ° 2 θ range, with a step of 0.002° and a λ equal to 1.540598 Å.

125 Water-sorption isotherms were measured by an intelligent dynamic vapor sorption
126 instrument (DVS Vacuum, SurfaceMeasurementSystems Ltd.) connected to a humidity
127 generator. The experiments were carried out in the temperature range of 20-60 °C at the
128 relative vapour pressure precisely (RH=0-95%). The humidity was controlled by using two
129 mass-flow controllers with dry air and pure vapour, respectively. The precise humidified
130 airflow passed through two thermogravimetric balances with the sample in one and blank
131 for another. Prior to the adsorption experiment, the samples were dehydrated at 150°C for
132 12 h under high vacuum ($< 10^{-6}$ torr).

133 1.2 Specific heat capacity

134 The specific heat capacity is directly linked to the thermal loss in an adsorption process
135 [33]. The DSC used in the experiment is μ SC, a Tian-Calvet type microcalorimeter
136 manufactured by Setaram Instrumentation, France. With this instrument, measurements can
137 be realized under isothermal conditions or with a constant heating rate ranging between

138 0.001 and 1.2 K/min. A schematic representation of the DSC is shown in Fig. 1. It has a
139 RMS noise level of 0.2 μ W typically. The temperature ranges from -20°C to 170°C,
140 controlled precisely by a Peltier element based thermostat, that surround the sample on all
141 sides. It is equipped with four calorimetric wells that enable two simultaneous tests for two
142 samples and two references. The measurement cell is made of Hastelloy C276 with an
143 internal volume of 850 μ L and is able to measure solid, liquid samples or blends. A bunch
144 of Peltier elements are positioned around the cell to measure the temperature difference
145 between the sample and the environment in 3D. This arrangement allows for measuring
146 thicker samples on larger volume closer to real conditions.



147 The determination of the specific heat capacity of MIL-160(Al) using the continuous
148 temperature programming method requires the realization of two different and successive
149 tests:

150 -a test with two empty cells (which will be called "blank");

151 -a test with the sample in the measurement cell and the reference cell remaining empty.

152 It is imperative to use the same "measurement" cell for both tests as well as an identical
153 temperature program.

154 To compare the impact of water sorption, both dry and fully loaded samples were measured.

155 For the loaded sample, before the test, the powder of MIL-160(Al) was saturated under an

156 air-vapor mixing flow of 30% RH at 20°C for 2 hours to ensure it achieved the uptake
157 equilibrium at this state. The sample was weighed and inserted into a batch cell. The
158 powder was carefully packed into the cell to ensure the homogeneity of the measured
159 sample. The initial mass was 400.85 mg.

160 The following experimental profile has been employed:

161 - stabilization at 20 °C during 1800s

162 - heating from 20 °C to 75 °C to 0.2 °C / min

163 - stabilization at 75 °C during 1800s

164 2.3 Thermal conductivity

165 Thermal conductivity is measured with a C-ThermTCi sensor from C-Therm, Canada. The
166 C-Therm TCi employs a modified Transient Plane Source technique. Instead of a common
167 used laser light heating source, a known current is applied to the sensor's spiral heating
168 element, providing a small amount of heat (Fig 2.). A guard ring around the sensor is
169 simultaneously charged to support a one-dimensional heat exchange between the primary
170 sensor coil and the sample. The current applied to the spiral element results in a rise in
171 temperature at the interface between the sensor and sample, which induces a change in the
172 voltage drop of the coil. The thermal diffusivity and conductivity is derived from the
173 temperature increasing curves versus heating time. The temperature increasing thus the
174 voltage rise is steeper for materials with lower thermal conductivity and flatter for higher
175 thermal conductivity.

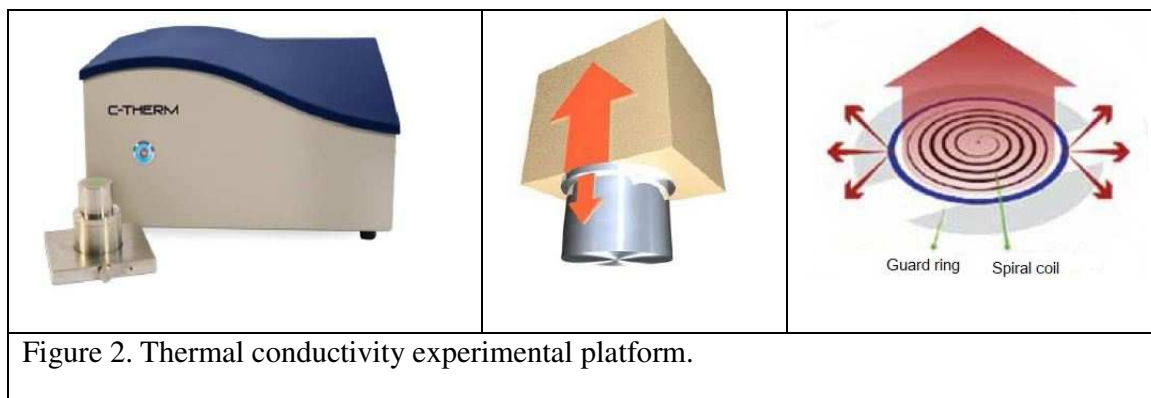


Figure 2. Thermal conductivity experimental platform.

176 The thermal conductivity is linked to the density of the sample. Powders of MIL-160(Al)
 177 have been compressed in to bloc under pressure. Again, a humid sample was obtained by
 178 saturating the packed powder under an air-vapor mixing flow of 30%RH at a lower
 179 temperature for 2 hours to ensure it achieved the loading equilibrium at this state. The
 180 whole analysis instrument was placed in a small climate chamber to regulate the RH. A dry
 181 sample for comparison was obtained by heating the humid sample under 90°C for 2 hours.

182 2. Results and discussion

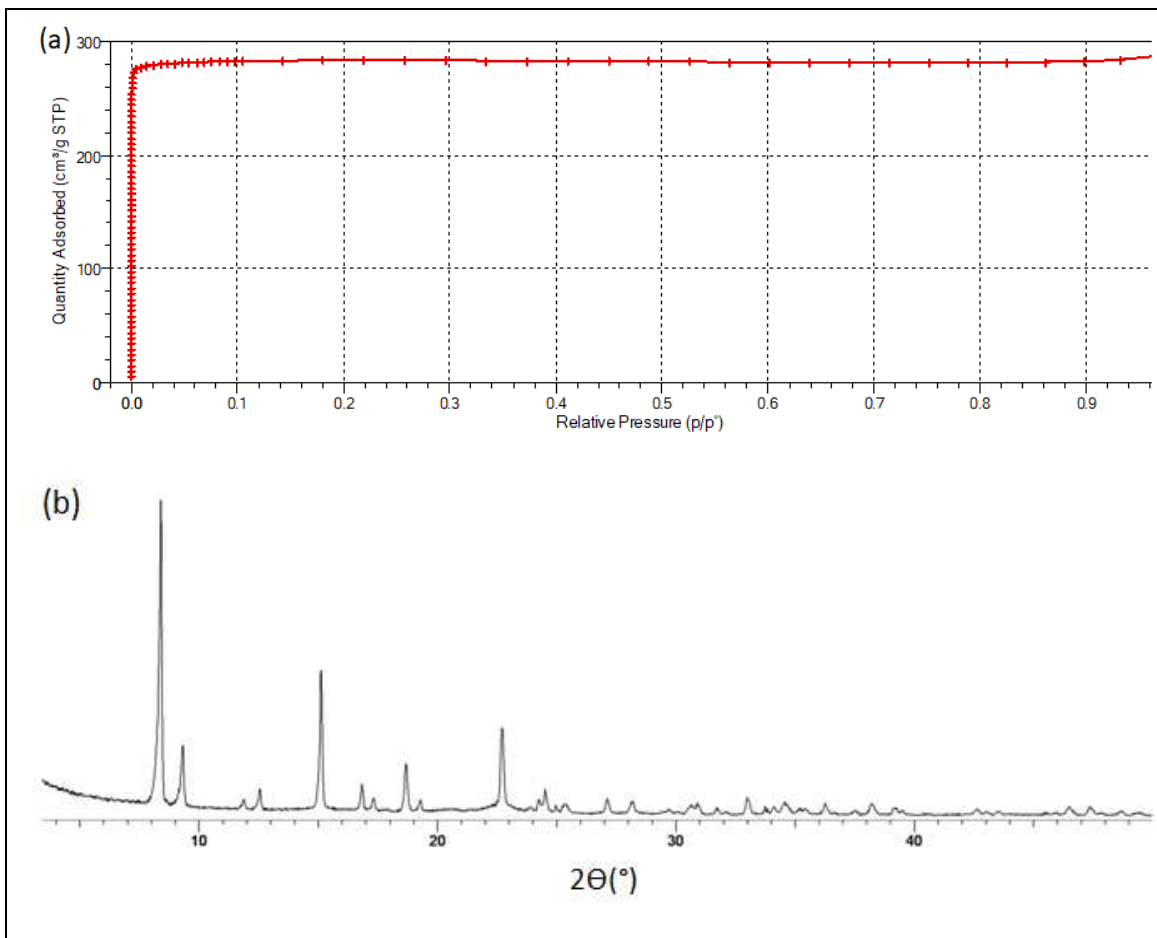
183 2.1 Characterization of MIL-160(Al)

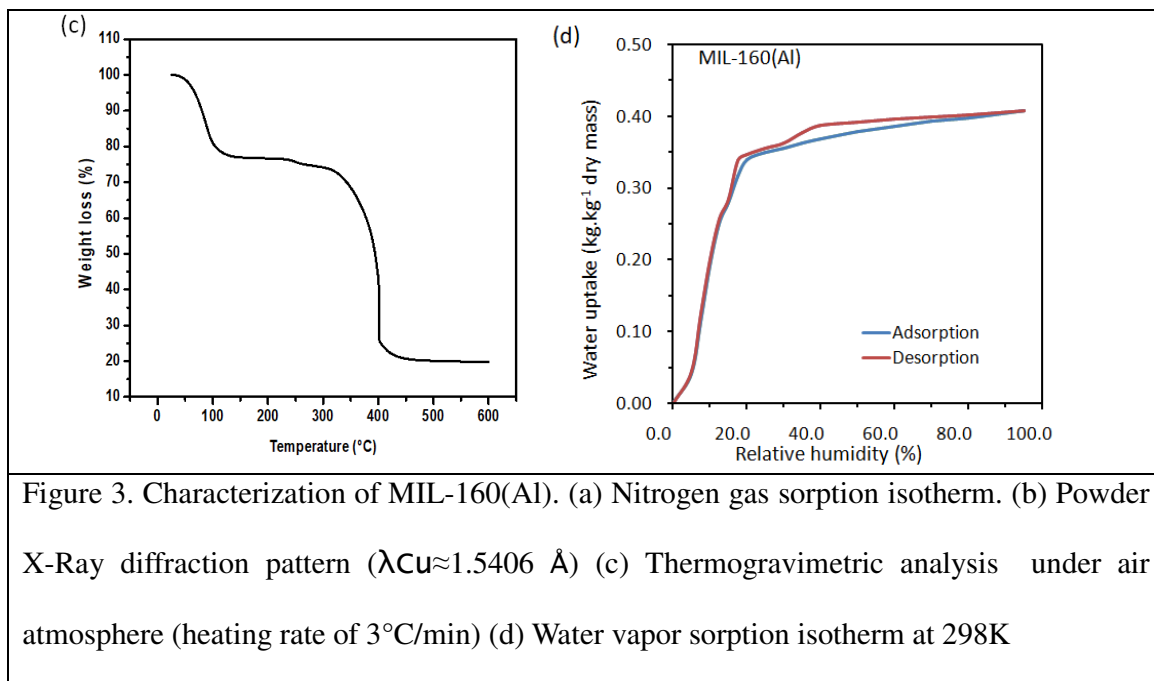
184 After purification and activation, the BET specific surface area and pore volume of the
 185 sample were found to be 1200 m²/g and 0.398 cm³/g respectively (Fig 3a).The PXRD
 186 pattern and thermalgravimetric of the MIL-160(Al) powder (Fig 3b,c) are consistent with
 187 previously synthesized with small scale process reported in [32]. Water adsorption
 188 isotherms for MIL-160 are step-wise curves with reflection point at around 8% P/P₀ and the
 189 majority uptake (>90%) is complete at 20% P/P₀ (Fig 3d). The position of adsorption stage
 190 varies very little under different temperature and can be neglected as we only focused on
 191 the full uptake conditions. The maximum uptake at P/P₀=0.9 reaches around 0.4 g/g dry
 192 mass. There is barely sorption hysteresis at all temperatures so that the adsorption and
 193 desorption routines almost coincide with each other which is an advantage to be integrated
 194 into an active mechanic system. The isosteric heat ΔH_{ads} of water adsorption can be

195 calculated from the adsorption isosteres according to the Clausius-Clapeyron relation,
196 given by [35]:

$$\Delta H_{ads}(T) = R \left(\frac{d(\ln P)}{d \left(-\frac{1}{T} \right)} \right)_w \quad (2)$$

197 Where ΔH_{ads} , R, P, T and w represent the isosteric enthalpy of adsorption, universal gas
198 constant, pressure, temperature, and water uptake. The isosteric enthalpy of adsorption is
199 obtained as a function of water uptake and adsorption isotherms measured across a wide
200 temperature range with a linear interpolation method. The ΔH_{ads} drops very quickly to 50
201 kJ/mol at the water uptake $w=0.02$ g/g dry mass, maintains this value until 0.3 g/g dry mass
202 and varies a little thereafter. This plateau of the ΔH_{ads} indicates reversible
203 adsorption-desorption phenomena.



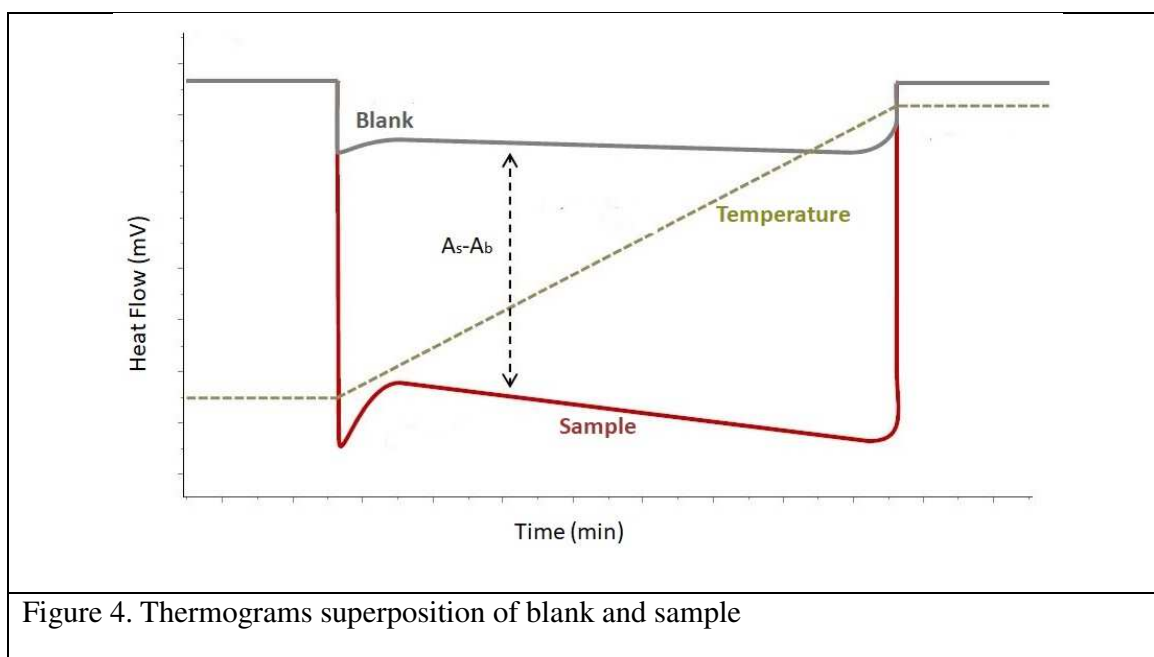


204

205 2.2 Specific heat capacity

206 The following idealized thermogram (Fig 4.) is obtained with the amplitudes of the Heat

207 Flow signal A_s and A_b (μV) at temperature T of the sample and blank, respectively.



208 The heat capacity of the sample can be calculated as the following equation:

| | |
|--|-----|
| $C_p(T) = \frac{A_s - A_b}{m_s \frac{dT}{dt}}$ | (1) |
|--|-----|

209 where $C_p(T)$ is the heat capacity of the sample in J/(g. K) at a temperature T; A_s and A_b are
 210 sample and blank output signals in μV ; m_s is mass of the sample in mg; $\frac{dT}{dt}$ is the heating
 211 rate in K/s.

212 The experimental conditions were adopted to measure a representative sample of 400 mg
 213 on macroscopic level and minimize the impact of the heating rate. The calculation of C_p
 214 was carried out from 20 to 75°C that is the operational temperature range of MIL-160(AI)
 215 for an adsorption heat pump system. The measured result of the highly loaded sample on
 216 each point of this temperature range is shown in Fig 5. The measured specific heat capacity
 217 remains almost constant with a slight increase by 3% over the temperature range.

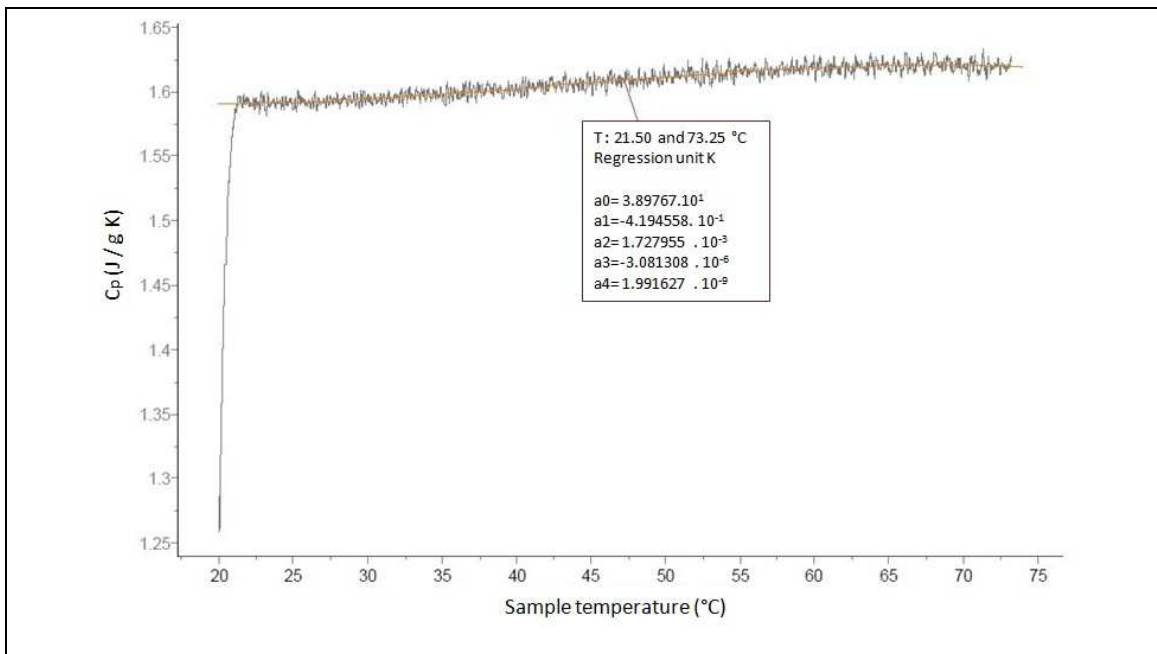


Figure 5. Evolution of the C_p of the sample between 20 °C and 75 °C

218 We listed the heat capacity of the dry material at a set of temperatures in Table 1 for the

219 comparison.

| Sample | 24.8 °C | 45.0 °C | 70.0 °C |
|---------------|---------|---------|---------|
| Highly loaded | 1.588 | 1.605 | 1.617 |
| Dry | 1.117 | 1.125 | 1.160 |

220 The more water the MOF contains, the higher its specific heat capacity. A reduction of 30%
221 on the C_p can be observed when the desorption is complete on the loaded sample. In a
222 typical thermodynamic cycle of the adsorption heat pump, the sorbents with higher water
223 uptake is often heated to desorption temperatures with external energy input and the
224 released heat during temperature decreasing is to be evacuated. The necessary energy cost
225 to power the cycling operation would be higher when using the heat capacity measured at
226 different uptake state than in a calculation based only on the value of dry materials.

227 2.3 Thermal conductivity

228 The thermal conductivity of the sample can be calculated from the following equation:

| | |
|------------------------|-----|
| $e = \sqrt{k\rho C_p}$ | (1) |
|------------------------|-----|

229 where e is the thermal effusivity in $W.s^{1/2}/(m^2.K)$, k is thermal conductivity in $W/(m.K)$, ρ
230 is the density in kg/m^3 .

231 The calculated thermal conductivity of one sample was shown in Table 2, which slightly
232 decreased with temperature increasing for each state of water uptake. The average values
233 are similar to conventional sorbents. The case of Loaded sample was saturated at 25°C and
234 30%RH. The relative humidity in the environment maintained at 30% when increasing the
235 temperature so that water uptake would not have an evident change. The case of Dry
236 sample was for dried adsorbent with less than 5%RH at different temperature. The case of

237 Open system was the saturated sample undergoing the increase of temperature in an open
 238 environment so that the RH decreased accordingly. As the saturated MIL-160(Al) can be
 239 completely regenerated below 90 °C in either open or closed mechanic systems, results at
 240 three typical temperatures were listed to demonstrate the measurement of its thermal
 241 conductivity: 25 °C, the hydrophilic MIL-160(Al) is easily saturated; 40°C, the vapour
 242 starts to be released in an open system; 70°C, desorption is complete in an open system A
 243 drop of thermal conductivity by 15% in average was obtained when vapour is completely
 244 desorbed from the saturated sample.

Table 2. Comparison of the thermal conductivity between dry and highly loaded samples,

| Sample 1 | 25.4 °C | | 43.6 °C | | 72.3 °C | |
|-------------|--|----------------------|--|----------------------|--|----------------------|
| | Effusivity (Ws ^{1/2} /m ² .K) | <i>k</i> (W/m. K) | Effusivity (Ws ^{1/2} /m ² .K) | <i>k</i> (W/m. K) | Effusivity (Ws ^{1/2} /m ² .K) | <i>k</i> (W/m. K) |
| Loaded | 172..173 | 0.071 | 160.732 | 0.069 | 157.723 | 0.068 |
| Dry | 131.356 | 0.061 | 129.141 | 0.061 | 127.240 | 0.060 |
| open system | 171.189 | 0.071 | 160.617 | 0.068 | 127.206 | 0.060 |

245 The packed density also impacts the thermal conductivity. The measured thermal
 246 conductivity of differently packed powder is shown in Table 3. The packed density and
 247 thickness was closed to the operational conditions where the effect due to macroscopic void
 248 volume was also taken into consideration.

249 Table 3. Impact of the compression force on the thermal conductivity

| | Temperature | Packed pressure | Test condition | <i>k</i> (W/m. K) |
|---------------------------|-------------|-----------------|----------------|----------------------|
| Loaded 1 | 25.4 °C | 3.5 kPa | loosely | 0.071 |
| Loaded 2 | 25.3°C | 3.5 kPa | 3.5 kPa | 0.078 |
| Loaded 3 | 25.3°C | 3.5 kPa | 12.95 kPa | 0.108 |
| Loaded 4 | 26.1°C | 3.5 kPa | 25.91 kPa | 0.117 |
| bead _{0.4-0.6mm} | 26.5°C | - | loosely | 0.065 |

250 The packed pressure of the powder layer was 3.5 kPa and the samples were tested with
 251 different level of external compression. A shaped sample under bead form with size of 0.4
 252 to 0.6 mm was shown to represent the realistic condition in the application of adsorption
 253 heat pump. The effective thermal conductivity of the beads is close to the loosely
 254 compacted powder which is a quite low value.

255 Since a low conductivity has a negative impact in the dynamic performance of the sorption
256 cycle, different strategies could be followed to improve the thermal efficiency, such as
257 packing the powder with higher bulk density, shaping the powder with variable binders (e.g.
258 silicate), and mixing in highly conductive additives (e.g. graphite, thermal conductivity
259 1400 w/(m. K), heat capacity 0.7 J/(g. K) in the same temperature range). However, the
260 additives will sacrifice the power density and energy storage density of the MOF in a
261 mechanic system, thus requiring further optimization in different working environment.
262 The pursuing in very high packed density is not recommended because of the drawback
263 that the mass transfer becomes weaker which lowers the specific power. In practice, it is
264 advised to coat the powder on the highly conductive surface to improve heat transfer.

265 2.4 Thermodynamic efficiency for adsorption cooler based on MIL-160(Al)

266 The above-measured values of adsorptive and thermal properties allow the accurate
267 calculation of the coefficient of performance (COP) for an adsorption cooler device based
268 on MIL-160(Al). The operational temperatures were chosen as 5°C for the evaporator,
269 30°C for the condenser and 85°C for the desorption process. The water adsorption isosteres
270 derived from the isotherms were mapped in to a Clausius – Clapeyron diagram as shown in
271 Fig. 5. The adsorbent exchanged water Δw by more than 30 wt% dry mass via a cyclic
272 sorption process. The hydrophilic nature enables a typical evaporation temperature of
273 5-7°C. The desorption temperature below 90°C allows the use of low-grade heat source.
274 MIL-160(Al) is approved as one of the most promising adsorbents for this application in
275 the literature.

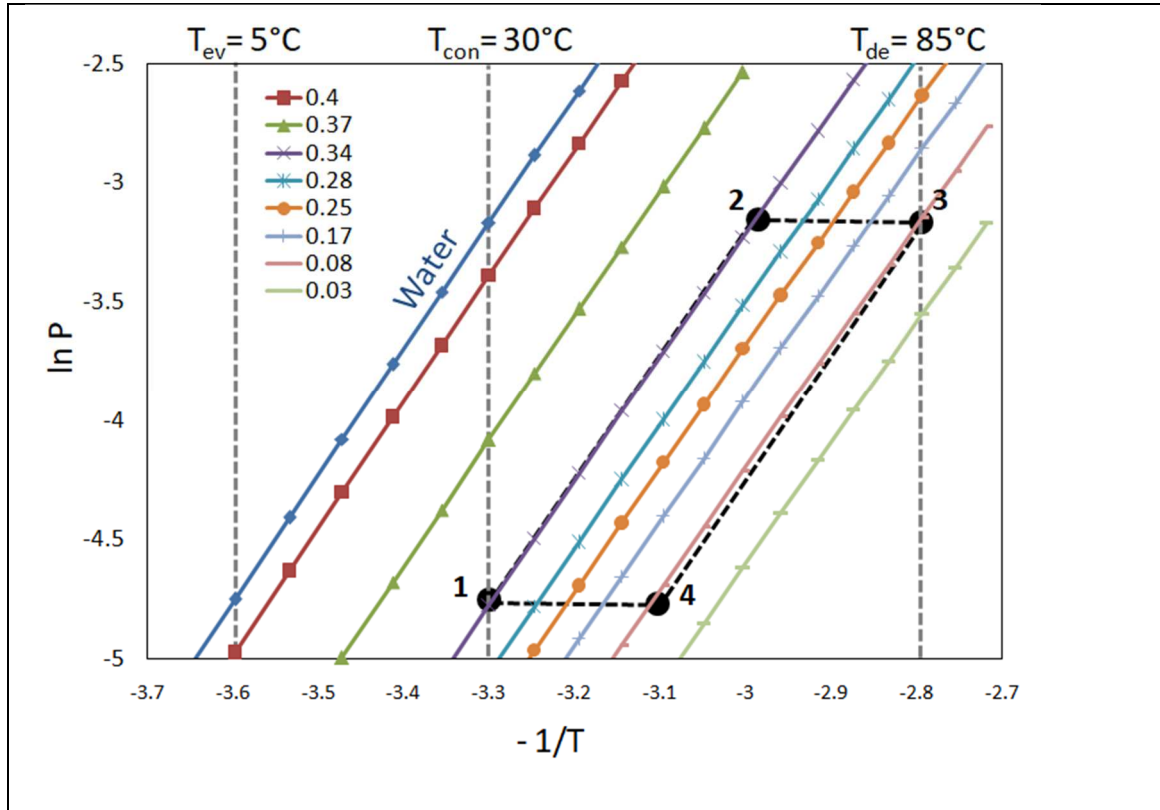


Figure 5. Water sorption isotherms of MIL-160(Al). Black dashed frameworks: adsorption cooling cycle at evaporation temperature (T_{ev}), condensation temperature (T_{con}) and desorption temperature (T_{de}) of 5/30/85°C. Water uptake w from 0.03 to 0.4.

276 The COP of the adsorption cooling cycle is calculated as the ratio of cold energy produced
 277 to the heat consumed during the isosteric heating and isobaric desorption [7].

$$\text{COP} = \frac{Q_{ev}}{Q_{ist} + Q_{de}} \quad (3)$$

278 This equation can be expressed as the refrigerant (water) evaporation heat over the sum of
 279 the specific heating process (Q_{ist}) and the latent heat of desorption process (Q_{de}). Assuming
 280 in adsorption and desorption, the adsorbent reaches thermodynamic equilibrium state at
 281 given temperature and pressure, the COP of the operational cycles of 5/30/85°C is 0.76. On
 282 the contrary, if the values of the heat properties were taken for the dry MOF, the
 283 corresponding calculation on the COP would render 0.79, with a positive deviation of 4%.
 284 The COP value makes MIL-160(Al) highly competitive to most conventional and
 285 innovative sorbents in the application of water adsorption cooling such as SAPO-34,

286 TAPSO and AIPO-18 [36].

287 **3. Conclusions**

288 In this work, a simple method that measures the heat properties of bulk porous materials is
289 applied on MIL-160(Al), an hydrophilic MOF highly performant in water vapor adsorption
290 processes. Both the thermal capacity and conductivity of the MOF was measured with high
291 resolution and accuracy in the common working range of an adsorption cooler. The specific
292 heat capacity of MIL-160(Al) demonstrated a slightly incremental tendency with
293 temperature. The heat capacity is undesirably higher than the commonly used zeolites such
294 as SAPO-34, TAPSO, and their thermal conductivity is quite close. However, this
295 difference has little impact on the COP of a thermal driven adsorption process given the
296 fact that the adsorption enthalpy is two orders of magnitude larger.

297 Since water adsorption was proven to become a more and more important subject in both
298 fundamental research and technology development thanks to the rapid development of
299 innovative sorbents, the method and protocol presented here will serve as a reference
300 technique to characterize the key thermal properties of the adsorbents in various sorption
301 systems.

302

303

304

305 **Acknowledgements**

306

307 **References**

308 [1] G. Maurin, C. Serre, A. Cooper, G. Ferey, The new age of MOFs and of their
309 porous-related solids. Chem. Soc. Rev. 46 (2017) 3104–3107,